Robust Optical Flow from Photometric Invariants

J. van de Weijer   Th. Gevers

Intelligent Sensory Information Systems
Faculty of Science, University of Amsterdam
Kruislaan 403, 1098 SJ Amsterdam, The Netherlands
{joostw, gevers}@science.uva.nl

Abstract

Optical flow is widely in use in the field of image processing. In general, optical flow is computed from luminance images. However, optical flow based on luminance information highly depends on moving shadows, varying shading and moving specularities due to camera movement, and fluctuations in the light source intensity.

In this paper, we propose a novel method to compute optical flow based on photometric invariants. A major drawback of photometric invariants and their derivatives is that they are unstable for certain RGB values. Therefore, we study on photometric invariant derivatives and noise propagation yielding a confidence measure indicating the stability of the corresponding photometric invariant derivatives. This confidence measure is integrated into the optical flow framework to provide robustness against noisy data.

Experimental results show that the proposed method significantly outperforms optical flow estimation that does not take the instability of the invariants into account.

1   Introduction

Optical flow is used as a low-level input for object motion estimation[6], [7]. In general, it is based on the brightness assumptions which states that points on the same object location (and hence the corresponding pixel values) have constant brightness over time. However, for real-world scenes varying lighting conditions, changing camera positions, moving shadows and changing intensity of the lightsource, all brake the brightness assumption.

A major advantage of color images is that they contain more photometric information. Based on the dichromatic reflection model of Shafer [8], photometric invariants with respect to shadows, shading and specularities can be derived. This allows for photometric invariant optical flow, which replaces the brightness assumption with a less restrictive constant chromaticity assumption, or a constant hue assumption.

Research on color optical flow acknowledged the advantage of photometric invariance [1] [2], [5]. A major drawback of photometric invariants is that they exhibit inherent instabilities [4]. E.g. the hue is unstable near the achromatic line.

In this paper, we derive reliability measures for each of the photometric invariants. This reliability is used to improve the photometric optical flow estimation. The novelty of the paper is the use of photometric invariants and the incorporation of the reliability measure within the optical flow framework to obtain robust object motion estimation even under severe illumination conditions and noisy data.

This paper is organized as follows. In section 2, multi-channel optical flow is described. Section 3 handles photometric invariants and their uncertainty. The uncertainty and the optical flow theory is combined in section 4. In section 5, experiments are given. Section 6 finishes with concluding remarks.

2   Multi Channel Optical Flow

In this section, we extend the optical flow of Lucas and Kanade [7] to the multi channel case. The vector of a multi-channel point over time stays constant [6]

$$\frac{d\mathbf{f}}{dt} = 0 \qquad (1)$$

with the multi-channel image $\mathbf{f} = \left(f^1, f^2, ..., f^n\right)^T$. Differentiating yields the following set of equations

$$\mathbf{f_x} \cdot \mathbf{v} + \mathbf{f_t} = \mathbf{0} \qquad (2)$$

with $\mathbf{f_x} = (f_x \ f_y)$ and the subscript indicates the derivative with respect to the used variable and $\mathbf{v}$ the optical flow. To solve the singularity problem and to robustify the optical flow computation we follow Simoncelli [9] and assume a constant flow within a Gaussian window. Solving equation 2 leads to the following optical flow equation

$$\mathbf{v} = \overline{(\mathbf{f_x}^T \mathbf{f_x})^{-1}} \ \overline{\mathbf{f_x}^T \mathbf{f}}_t = \mathbf{M}^{-1}\mathbf{b} \qquad (3)$$

where

$$\mathbf{M} = \left(\begin{array}{cc} \overline{\mathbf{f}_x^T \mathbf{f}_x} & \overline{\mathbf{f}_x^T \mathbf{f}_y} \\ \overline{\mathbf{f}_y^T \mathbf{f}_x} & \overline{\mathbf{f}_y^T \mathbf{f}_y} \end{array} \right) \qquad (4)$$

and

$$b = \left(\begin{array}{c} \overline{\mathbf{f}_x^T \mathbf{f}_t} \\ \overline{\mathbf{f}_y^T \mathbf{f}_t} \end{array} \right). \qquad (5)$$

The bar $\bar{\cdot}$ indicates the convolution with a Gaussian filter

3 Photometric Invariants

In this section we describe a number of invariants. A drawback of using invariants is that they are unreliable due to instabilities. Therefore we propose a certainty measure to accompany the invariants. First the dichromatic reflection model is described which allows us to derive the invariants.

3.1 Dichromatic Reflection Model

The dichromatic model divides the reflection in the interface (specular) and body (diffuse) reflection component for optically inhomogeneous materials. We assume white illumination, i.e. smooth spectrum of nearly equal energy at all wavelengths, and neutral interface reflection. The RGB vector, $\mathbf{f} = (R, G, B)^T$, can be seen as a weighted summation of two vectors,

$$\mathbf{f} = e(m^b \hat{\mathbf{c}}^b + m^i \hat{\mathbf{c}}^i) \qquad (6)$$

in which $\hat{\mathbf{c}}^b$ is the color of the body reflectance, $\hat{\mathbf{c}}^i$ the color of the interface reflectance (i.e. specularities or highlights), m^b and m^i are scalars representing the corresponding magnitudes of reflection and e is the intensity of the light source. Note that the hat, $\hat{\cdot}$, is used to denote unit vectors. For matte surfaces there is no interface reflection and the model further simplifies to

$$\mathbf{f} = e m^b \hat{\mathbf{c}}^b \qquad (7)$$

which is the Lambertian reflection. For more on the validity of the photometric assumptions see [3], [8].

3.2 Photometric Invariants

In this section we look at two other colorspaces which can also be used for optical flow.

An photometric invariant colorspace with respect to shadow-shading changes is the $\theta\varphi$-space which can be found after a spherical coordinate transformation of the RGB coordinates

$$\begin{array}{l} r = \sqrt{R^2 + G^2 + B^2} = |\mathbf{f}| \\ \theta = \arctan(\frac{G}{R}) \\ \varphi = \arcsin\left(\frac{\sqrt{R^2+G^2}}{\sqrt{R^2+G^2+B^2}} \right) \end{array}. \qquad (8)$$

Here both the θ and the φ are invariant for shadow and shading changes for Lambertian reflection. This can be proven by substituting eq. 7 in 8 after which the terms e and m^b drop out. For the computation of distances (and hence derivatives) the scale factors of the spherical coordinate transformation should be taken into account.

$$\mathbf{f}_x = \left(\begin{array}{c} r_x \\ r\varphi_x \\ r\sin\varphi\,\theta_x \end{array} \right) = \left(\begin{array}{c} r_x \\ 0 \\ 0 \end{array} \right) + r \left(\begin{array}{c} 0 \\ \varphi_x \\ \sin\varphi\,\theta_x \end{array} \right) \qquad (9)$$

The last part of this equation we will use as a shadow-shading invariant derivative

$$\mathbf{c}_x = \left(\begin{array}{c} 0 \\ \varphi_x \\ \sin\varphi\theta_x \end{array} \right) \qquad (10)$$

We will use the opponent colorspace

$$\begin{array}{l} o1 = \frac{R-G}{\sqrt{2}} \\ o2 = \frac{R+G-2B}{\sqrt{6}} \\ o3 = \frac{R+G+B}{\sqrt{3}} \end{array} \qquad (11)$$

to derive the hsi colorspace

$$\begin{array}{l} h = \arctan\left(\frac{O1}{O2}\right) \\ s = \sqrt{O1^2 + O2^2} \\ i = O3 \end{array}. \qquad (12)$$

The hue h is a well known photometric invariant with respect both to shadow-shading and specular reflectance. This can be proven by substituting eq. 6 in eq. 12 after which e, m^b and m^i all cancel out. For the computation of derivatives in hsi space one should take the scale factors of the polar transformation into account.

$$\mathbf{f}_x = \left(\begin{array}{c} sh_x \\ s_x \\ i_x \end{array} \right) = \left(\begin{array}{c} 0 \\ s_x \\ i_x \end{array} \right) + s \left(\begin{array}{c} h_x \\ 0 \\ 0 \end{array} \right) \qquad (13)$$

The derivative of the hue

$$\mathbf{h}_x = \left(\begin{array}{c} h_x \\ 0 \\ 0 \end{array} \right) \qquad (14)$$

is used in this article for shadow-shading and specular invariant optical flow estimation.

3.3 Uncertainty of the Invariants

Photometric invariants have inherent instabilities due to the transformation to obtain these photometric invariants e.g. the invariants for shadow-shading are unstable around the intensity of zero. The invariants for shadow-shading and
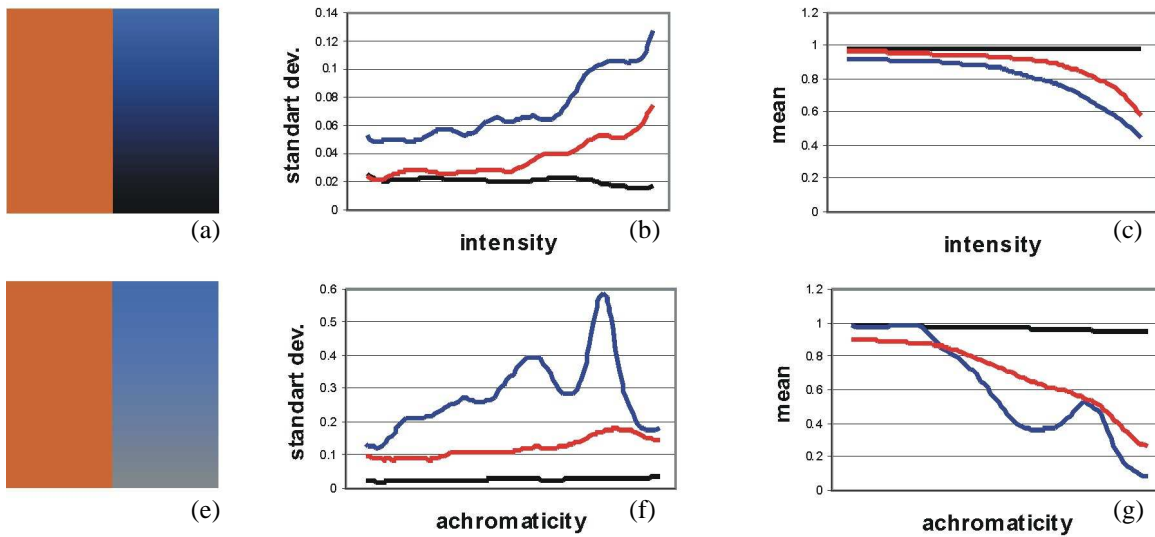
Figure 1: a) test edge with decreasing intensity. b,c) standard deviation and mean of the optical flow based on RGB (black line), shadow-shading invariant (blue line) and robust shadow-shading invariant (red line). d) test edge with increasing achromaticity. e,f) standard deviation and mean of the optical flow based on RGB (black line), shadow-shading and specular invariant (blue line) and robust shadow-shading and specular invariant (red line).

specularities are unstable round the gray axis, which is the axis consisting of points with equal RGB values. These instability greatly reduce the applicability of the invariant derivatives where a small deviation of the original pixel value may result in a large deviation in the transformed value. In this section, we study on the reliability of the invariant derivatives by means of error propagation. The goal is to couple a certainty measure to each invariant derivative measurement.

If we assume additive uncorrelated uniform Gaussian noise then the derivatives of the RGB will also be uniformly distributed. After an orthogonal transformation and taking the scaling factors into account this noise is still uniformly distributed for each of the channels, hence

$$r\hat{\mathbf{c}}_x = \begin{pmatrix} 0 \\ \varphi_x \\ \sin\varphi\theta_x \end{pmatrix} \pm \begin{pmatrix} \sigma_r \\ \sigma_\varphi \\ \sigma_\theta \end{pmatrix} \qquad (15)$$

with $\sigma_r = \sigma_\varphi = \sigma_\theta$. The invariant $\mathbf{c}_x$ can now be written as

$$\hat{\mathbf{c}}_x = \begin{pmatrix} 0 \\ \varphi_x \\ \sin\varphi\theta_x \end{pmatrix} \pm \frac{1}{r}\begin{pmatrix} \sigma_r \\ \sigma_\varphi \\ \sigma_\theta \end{pmatrix} \qquad (16)$$

and hence the standard deviation of the measurement of $\mathbf{c}_x$ is inversely proportional with $r = |\mathbf{f}|$.

A similar derivation results in the standard deviation of the derivative of the hue to be inversely proportional with the saturation.

4 Combining Certainty and Optical Flow

In this section we will combine the color optical flow from section 2 with the photometric invariants, hereby constructing robust photometric optical flow. The standard deviation of the invariants will be used as a weighting factor.

The assumption of color optical flow based on RGB is that the RGB pixel values remain constant over time (see eq.1). A change of brightness introduced due to a shadow, or a lightsource with fluctuating brightness such as the sun results for this intensity constraint in non existent optical flow. This problem can be overcome by assuming constant chromaticity over time.

As discussed before the standard deviation of derivative in the chromaticity sphere is inversely proportional with $r = |\mathbf{f}|$. We therefor weigh the derivative vectors within the local window accordingly, e.g. the second matrix element of eq. 4 becomes

$$\frac{\overline{r^2\mathbf{c}_x^T\mathbf{c}_y}}{\overline{r^2}} = \frac{\overline{r^2\left(\varphi_x\varphi_y + \sin^2\varphi\theta_x\theta_y\right)}}{\overline{r^2}} \qquad (17)$$

The other matrix elements in eq. 4 and 5 can be replaced with similar expressions after which the shadow invariant optical flow is computed with eq. 3.

For specular object a change of the lightsource direction results in both moving shadows and moving specularities, thereby falsely influencing the measured optical flow. This
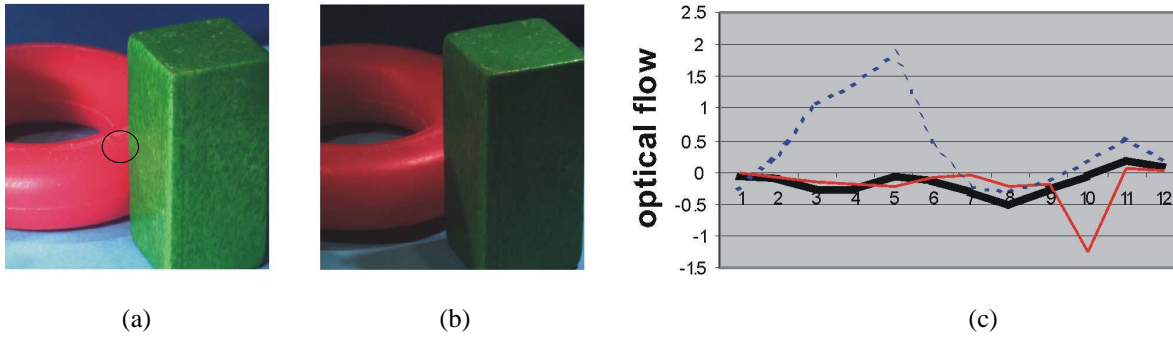
3

Figure 2: a) frame 1 with filtersize superimposed on it b) frame 10 c) estimated optical flow over time on the x-position which is indicated in a), with RGB (dotted line), shadow-shading invariant (red line), and shadow-shading and specularity invariant (thick black line).

can be overcome by applying hue based optical flow. In section 3.3 the deviation of the hue is shown to be inversely proportional to the saturation. The saturation is therefor applied as weight for hue based optical flow, e.g.

$$\frac{\overline{s^2 \mathbf{h}_x^T \mathbf{h}_y}}{\overline{s^2}} = \frac{\overline{s^2 h_x h_y}}{\overline{s^2}}. \tag{18}$$

5   Results

The shadow-shading photometric optical flow is tested on a synthetical image sequence. A test image with decreasing intensity (see fig. 1a)) is shifted one pixel per frame. Uncorrelated Gaussian noise with $\sigma = 20$ is added to the sequence. The derivatives are computed with a Gaussian derivative kernel at scale $\sigma = 1$ and for the local neighborhood a Gaussian of scale $\sigma = 5$ is chosen. In fig. 1b,c the mean and the standard deviation of the optical flow along the y-axis of fig.1a are depicted. Similarly the shadow-shading and specular invariant optical flow is tested on a sequence with increasing achromaticity along the axes (see fig.1d,e,f.). The results show that the optical flow methods which take the reliability of the measures into account (red lines) outperform the standard photometric optical flow (blue lines). Especially the difference for the standard deviation is striking; the improvement is more than a factor two for almost all the measured points.

As an example of a real-world scene, multiple frames are taken from two objects while the lightsource position is changed. This results in a violation of the brightness constraint by the moving shadows and specularities. Since both the camera and the objects did not move the ground truth optical flow is zero. Two of the frames of the sequences are depicted in fig. 2a) and b). Fig. 2c. shows the estimated optical flow for the point indicated in 2a). The violation of the brightness constraint can clearly be seen in the optical flow estimation based on the RGB. The shadow-shading

invariant optical flow remains near zero over the frames, except for frame 10 where a specularity violates the constant chromaticity constraint. The hue-based optical flow is not influenced by the shifting specularity.

6   Conclusions

In this paper we proposed a method for photometric invariant optical flow. This allows for a more realistic model including events such as moving shadows, varying shading and shifting specularities due to camera movement, and fluctuations in the light source. The instabilities of the photometric invariants are investigated and a reliability measure is proposed. Results show that the robust photometric optical flow significantly outperforms the standard optical flow.

References

[1] R.J. Andrews and B. C. Lovell. Color optical flow. In *Eds. Proceedings Workshop on Digital Image Computing*, Brisbane, 2003.

[2] J. Barron and R. Klette. Quantitative color optical flow. In *Int. Conf. on Pattern Recognition*, pages 251–255, Vancouver, Canada, 2002.

[3] J.M. Geusebroek, R. van den Boomgaard, A.W.M. Smeulders, and H. Geerts. Color invariance. *IEEE Trans. Pattern Analysis Machine Intell.*, 23(12):1338–1350, 2001.

[4] Th. Gevers and H.M.G. Stokman. Robust histogram construction from color invariants for object recognition. *IEEE Trans. Pattern Analysis and Machine Intelligence*, 26:113–118, 2004.

[5] P. Golland and A. M. Bruckstein. Motion from color. *Computer Vision and Image Understanding*, 68(3):346–362, December 1997.

[6] B. K. P. Horn and B. G. Schunk. Determing optical flow. *Artificial Intelligence*, 17:185–203, 1981.

[7] B. Lucas and T. Kanade. An iterative image registration technique with an application to stereo vision. In *Proc. DARPA Image Understanding Workshop*, pages 121–130, 1981.

[8] S.A. Shafer. Using color to seperate reflection components. *COLOR research and application*, 10(4):210–218, Winter 1985.

[9] E. P. Simoncelli, E.H. Adelson, and D.J. Heeger. Probability distributions of optical flow. In *IEEE conference on Computer Vision and Pattern Recognition*, pages 310–315, 1991.